MODELING OF HYDRODYNAMICS OF SUB-SEA FLOATING STRUCTURES FOR MOLLUSC OFFSHORE CULTIVATION

Bruno Galler Kubelka

Claudio Rodrigues Olinto

Waldir Terra Pinto

kubelkabruno@gmail.com

crolinto@gmail.com

waldirpinto@furg.br

Engineering School - Federal University of Rio Grande (FURG)

Av. Itália, km 08. Carreiros - Rio Grande, RS - Brazil - 96201-900

Walter Jesus Paucar Casas

walter.paucar.casas@ufrgs.br

Engineering School - Federal University of Rio Grande do SUL (UFRGS)

Rua Sarmento Leite, 425. Cidade Baixa - Porto Alegre, RS - Brazil - 90050-170

Abstract. *The increase in cultivated mollusc production have been limited by several obstacles in it development in coastal areas. The expansion of these farms to offshore regions may mitigate many of those problems. For that, structural and biological aspects of mollusc cultivation need improvements.. Numerical simulations of a computational wave flume were done using a commercial program, STAR-CCM+. The drag force coefficient of the droppers and the water velocity around it, resulting from a fifth order unidirectional wave, were analyzed in four different depths. Drag coefficient was reduced in a higher depth of the cultivation structure. Also, water velocity around the droppers was suggested less hostile to filtration of molluscs in the case of higher depth.*

Keywords: *mollusc cultivation, offshore farm, Computational Fluid Dynamics, filtration rate, drag coefficient.*

1 INTRODUCTION

World marine aquaculture mollusc production was approximately 16 tons in the year of 2015 (FAO, 2017). Most of farms in operation are near the coast. Yet, increasing production in coastal areas has become harder as space conflicts are numerous. For example, space sharing with navigation, highly contaminated effluents discharge and for an intensive cultivation higher water circulation is necessary to prevent water quality degradation and seston continuous supply for bivalve filtration (Strohmeier et. al., 2005). First two should be mitigated by installation of the farm a few miles offshore. Water movement around and through the farm certainly will be higher in offshore farms, what should benefit water conditions around the droppers and should aid molluscs growth.

Molluscs bivalves (pair of shells) are cultivated in horizontal lines (long-lines) with droppers vertically oriented remembering a set of suspended cylinders (Plew, 2005). The organism opens its shell and water circulates inside the shells allowing filtration of the microalgae present in the water column (Plew, 2009). So, feeding and growth of the bivalve are related with water flow velocities around it (Pilditch and Grant, 1999). Better cultivation conditions should result in higher meat content (Strohmeier et. al., 2005). The drawback from moving farms offshore is the hydrodynamic implication from much severe waves, winds and currents than in coastal zone. These environmental conditions should be even more troublesome taking in account the standard depth that shellfish farms are installed, 0.25-0.50 meters from ocean surface (Marenzi and Branco, 2006; Li et. al., 2016).

Current study evaluated the flow resulting from progressive waves as a start point for avoiding high hydrodynamic loads in cultivation structure and for improving mollusc growth conditions. Higher cultivation structure depth installation was analyzed for the drag force coefficient and the water velocity around the droppers. Commercial Computational Fluid Dynamics program was utilized to predict wave load and water velocity field for two different cultivation depths.

2 METHODS

2.1 Numerical domain

Geometry and mesh

Wave flume geometry was matched with the experimental flume in Laboratory of Fluid Structure Interaction from Federal University of Rio Grande, Brazil. Flume was developed in the 3D CAD included in the commercial software STAR-CCM+ 12.02. Water column (h) was set to 0.60 m, width was 0.71 and length was 12.00 m (Figure 1 (a)). Vertical cylinders (droppers) dimensions are shown in Table 1, as well a typical full scale droppers dimension used in mollusc bivalve cultures in Brazil. Proportion between laboratory and full scale was 1:10 m.

Mesh generation was also done using the STAR-CCM+ interface (Figure 1). Table show 2 mesh characteristics. Mesh quality was verified by a tool included in STAR-CCM+, Mesh Diagnostics, and all requests for a satisfactory mesh were attended in both cases (CD-adapco, 2017).

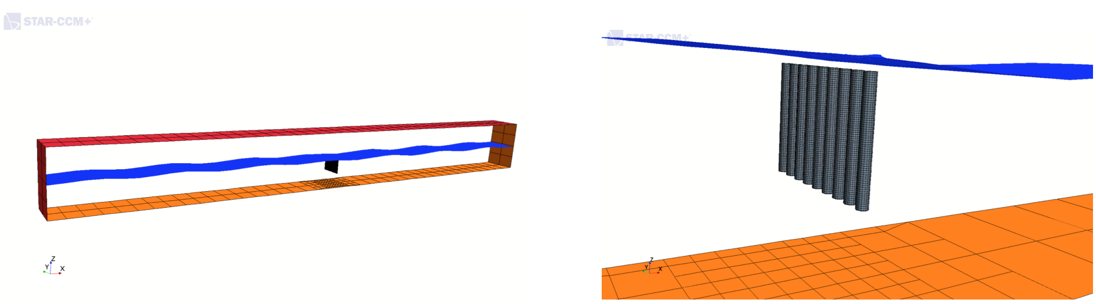

(a) (b)

Figure 1: (a) Geometry, mesh and boundary conditions for case 1. Case 2 mesh was not shown given its similarity to case 1 mesh. (b) Mesh refinement close to the droppers (cylinders).

Table 1: Structure characteristics comparing the simulated laboratory scale with the full-size dimensions. D_D is the dropper diameter, l_D is the dropper length and d_S corresponds to the initial depth that the structure is installed.

Scale	D_D (m)	l_D (m)	d_S (m)
Full	0.30	3.00	0.25/1.00
Laboratory	0.03	0.30	0.025/0.10

Table 2: Number of cells (NC) and minimum cell size (MCS) for each simulation case. T is the total tie of simulation and d_S is the initial depth that the structure is installed.

Case	NC	MCS (m)	T (s)	d_S (m)
1	61,896	$6.0e^{-4}$	34	0.025
2	53,348	$6.0e^{-4}$	34	0.10

Boundary conditions and initial conditions

The tank did not present any wave propagating through the water column at the beginning of the simulation, there is water was at rest. As the transient simulations runs, waves enter through inlet (Figure 1 (a)). Wave height and length are shown in Table 3. It propagates until the center of the computational flume, where cylinders walls start to separate the wave motion. At the flume end a pressure outlet is present, also the bottom is attributed as pressure outlet so wave acts as deep waves and do not interact with the flume bottom (Figure 1 (a)). Shear stress on the side walls in the flume were set as slip (CD-adapco, 2017).

Table 3: Wave height (H) and length (L) utilized in the simulations of a fifth order unidirectional wave model. Water column height value is shown also (h).

Wave model	H (m)	L (m)	h (m)
Fifth order	0.10	1.70	0.60

2.2 Numerical Models

The Computational Fluid Dynamics (CFD) was employed for solving fluid dynamics equations. Air-water interactions of the free surface were considered as multiphase problems, where fifth order water waves were simulated. To predict water circulation resulting from the wave passage through the flume, STAR-CCM+, a CFD commercial program, was used. Through the Multiphase Segregated Flow model a set of conservation equations for both Eulerian phase (air and water) was solved (CD-adapco, 2017). And, air-water interactions were solved by the Volume of Fluid wave model.

Fluid dynamics equations

The following integral equation (Equation 1) represent Navier-Stokes equations for continuity and momentum for each phase (Newman, 1977):

$$\frac{\partial}{\partial t}\left(\int_V \rho\mathbf{v}\right) dV + \int_A \rho\mathbf{v}\otimes(\mathbf{v}-\mathbf{v}_g)\, d\mathbf{a} = -\int_A p\mathbf{I}\cdot d\mathbf{a} + \int_A \mathbf{T}d\mathbf{a} + \int_V \mathbf{F}dV \tag{1}$$

Where t stands for time, V is the cell volume, ρ is phase density, $\mathbf{v}$ is the velocity vector, $\mathbf{v}_g$ is the grid velocity vector, $\mathbf{a}$ is the face area vector, p is the pressure, $\mathbf{I}$ is the identity matrix, $\mathbf{T}$ is the viscous stress tensor and $\mathbf{F}$ represents all body forces that should be incorporated to the equation to be solved.

From Equation 1 Finite Volume Discretization method was applied to solve the equation numerically. Current simulations used first order temporal discretization with a $1.0E^{-2}$ time-step and velocity convection was accounted on second order. Solver SIMPLE algorithm was used to control the overall solution (CD-adpaco, 2017).

Turbulence models

Navier-Stokes equations for the instantaneous velocity and pressure fields were decomposed into a mean value and a fluctuating component, resulting on equations for the mean quantities that are identical to the original equations, except that an additional term now appears in the momentum transport equations. This additional term is a tensor quantity, c the Reynolds stress tensor ($\mathbf{T}$), which has the definition of Equation 2 (Ferziger and Perić, 2002):

$$\mathbf{T} = -\rho\begin{pmatrix}\overline{u'u'} & \overline{u'v'} & \overline{u'v'}\\ \overline{u'v'} & \overline{v'v'} & \overline{v'w'}\\ \overline{u'w'} & \overline{v'w'} & \overline{w'w'}\end{pmatrix} \tag{2}$$

A Standard K-Epsilon turbulence model was selected to provide predicted turbulence solutions from the governing equations. Transport equations were solved for turbulent kinetic energy (k) and its dissipation rate (ϵ) as can be seen on Equations 3 and 4 (Wilcox, 2000).

$$\frac{\partial k}{\partial t} + U\frac{\partial k}{\partial x} = \mathbf{T}\frac{\partial U}{\partial x} - \epsilon + \frac{\partial}{\partial x}\left[\left(\frac{\nu+\nu_T}{\sigma_k}\right)\frac{\partial k}{\partial x}\right] \tag{3}$$

$$\frac{\partial \epsilon}{\partial t} + U\frac{\partial \epsilon}{\partial x} = C_{\epsilon 1}\frac{\epsilon}{k}\mathbf{T}\frac{\partial U}{\partial x} - C_{\epsilon 2}\frac{\epsilon^2}{k} + \frac{\partial}{\partial x}\left[\left(\frac{\nu + \nu_T}{\sigma_\epsilon}\right)\frac{\partial \epsilon}{\partial x}\right] \tag{4}$$

Where $C_{\epsilon 1}$ was set to 1.44, and $C_{\epsilon 2}$ to 1.92, these are the model closure coefficients defined on literature (CD-adapco, 2017; Wilcox, 2000). U corresponds to the mean velocity for the position x. ν is kinematic velocity coefficient of the fluid that the particle is immersed and ν_T is the kinematic eddy viscosity.

Volume of fluid waves

A fifth order wave is modeled with a fifth order approximation to the Stokes theory of waves. This wave more closely resembles a real wave than a wave that is generated by the first order method. The wave profile and the wave phase velocity depend on the water depth and wave height. The fifth order volume of fluid waves are based on work by Fenton (1985).

2.3 Hydrodynamic evaluation

The wave propagation through the domain and its momentum transfer to the water column results in hydrodynamics forces exerted on cylinder walls. The Drag force (D) has been suggested as the most important force acting in full scale mollusk farms (Lin et al., 2016; O'Donncha et al., 2013). Therefore, it was used to compare the hydrodynamic performance of a set of nine cylinders, remembering a long-line of mollusk droppers, in two different installation depths of the water column.

In the dimensional form, shown in Equation 5, each cylinder D is in function of the diameter d, the upstream flow velocity (U), water density (ρ) and the kinematic viscosity coefficient ν:

$$D = f(d, U, \rho, \nu) \tag{5}$$

Nondimensionalizing these five parameters yields two nondimensional quantities, which can be expressed in the form shown in Equation 6:

$$\frac{D}{\frac{1}{2}\rho d^2} = f(\frac{Ud}{\nu}) \tag{6}$$

Where $R = Ud/\nu$ is the Reynolds number based on the cylinder diameter.

In this analysis the body weight and buoyancy force are not involved because we are considering only the hydrodynamic drag force associated with steady translation of the body. There fore a Drag Coefficient (C_D) can be determined by the equation :

$$C_D(R) = \frac{D}{\frac{1}{2}\rho U^2 S} \tag{7}$$

Where S is the frontal area of the cylinder.

2.4 Biological constraint of water flow around droppers

Marine mussel cultivation is mainly with filtering organisms, as scallops, mussels and clams. Most are suspended in the water column exposing it to momentum transfer from waves, currents and winds. Although the presence of those forcing agents aids for filtration rate (or clearance rate), exists a flow velocity limit for the organism to stop the feeding (Table 4). Studies of these physical-biological interaction are scarce and far from knowing the optimum flow conditions for all cultured bivalve species. We utilized those values in Table 4 for comparing with the two cases here simulated of water velocity field around droppers. All these estimations assumed that water column microalgae concentrations are constant.

We monitored water velocity in eight points for each simulation case, four points around the center dropper and four points around a dropper closer to the wall.

Table 4: Four studies with three mollusc bivalve species of water velocity effect in filtration. v_o is the optimum velocity for organism growth and v_i is the velocity in which filtration is inhibited.

negrito Study	Species	Common name	v_o $(m.s^{-1})$	v_i $(m.s^{-1})$
Newell et al. (2001)	*Mytilus edulis*	Blue mussel	0.10	0.3
Sobral & Widdows (2000)	*Ruditapes decussatus*	Clam	0.08	0.16
Pilditch & Grant (1999)	*Placopecten magellanicus*	Scallop	0.05-0.15	0.25
Wildish & Sauliner (1993)	*Placopecten magellanicus*	Scallop	0.03-0.06	0.3

3 Results and Discussion

3.1 Drag Coefficient

In Table 5, drag coefficient was lowest in case 1 than case 2. Positioning the cultivation structure deeper should reduce wave loads in the droppers. Although, the reduction in the drag coefficient was small in laboratory scale, we suggest as the scales becomes closer to full scale these difference in drag coefficient should become more evident.

Table 5: Maximum drag force coefficient from all droppers in each simulation case.

Cases	C_D
1	1.65
2	1.55

3.2 Biological constraint of water flow

Bivalves filtration activities are related with flow velocity around it, if seston (microalgae and other feeding microorganisms) concentrations are not low (not been the limiting factor). In

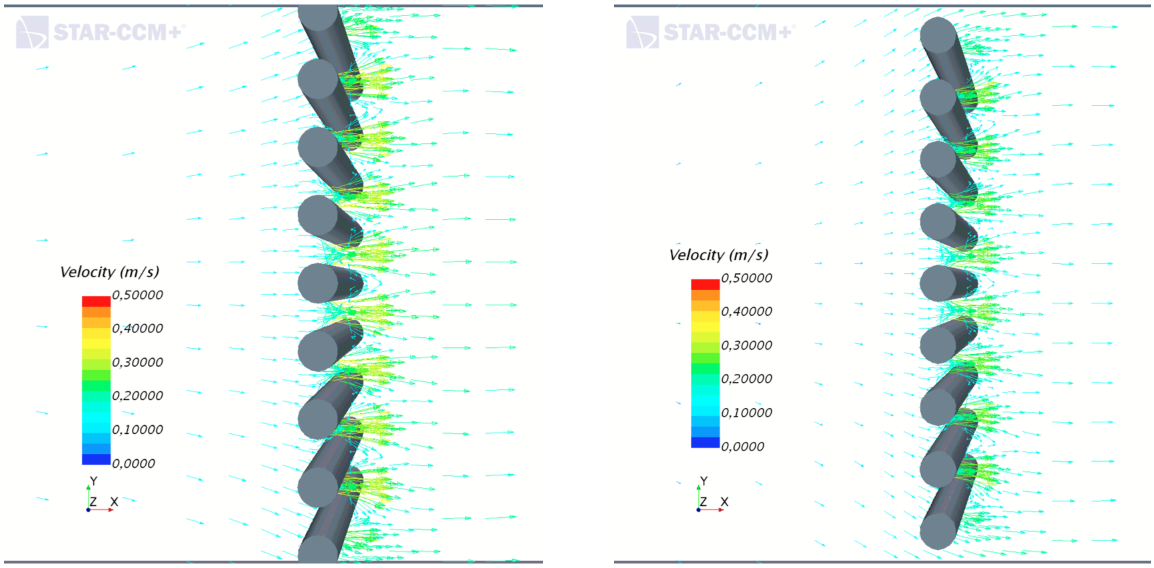

(a) (b)

Figure 2: Both case maximum water velocity field (a) Case 1 (lower depth); (b) Case 2 (higher depth).

Table 6: Maximum velocity observations in eight probes (p1,p2,p3,p4,p5,p6,p7,p8). All point probes velocity is shown in units of $m.s^{-1}$.

Case	p1	p2	p3	p4	p5	p6	p7	p8
1	0.1052	0.1459	0.1413	0.3462	0.1413	0.1129	0.2322	0.3419
2	0.1039	0.1407	0.1345	0.3245	0.1356	0.1087	0.21	0.3173

Figure 2 and Table 6 water velocity around the cultivation structure (set of droppers) are shown for both simulation cases.

Flow field patterns for both cases are similar, water acceleration was verified in the spacing among cultivation droppers (cylinders). However, intensities between case 1 (Figure 2 (a)) and case 2 (Figure 2 (b)) are different. Case 1 showed higher velocities than Case 2 for all points monitored (Table 6). Maximum velocity was 0.3462 $m.s^{-1}$ in case 1 and 0.3245 $m.s^{-1}$ in case 2, for both cases filtration should be inhibited for all organisms evaluated (Table 4). From Table 6 we observed that p1 and p4 velocities were optimum for the Blue Mussel. Simply by, installing the cultivation structure 0.075m deeper (laboratory scale), we observed that filtration inhibition can be avoided is structure is installed even deeper. As suggested for drag coefficient a third case, higher depth, may result in optimal water velocities for filtration activities for the cultivated molluscs.

4 Conclusions

Two mollusc cultivation structures were compared, in the first case droppers were positioned closer to wave action in the water surface, and in the second case droppers was positioned 0.075 m deeper (laboratory scale). Drag coefficient slightly reduced in the case with deeper positioning, and water velocity was moderately lower. These findings add each other to suggest that offshore mollusc cultivation can be installed deeper than traditional depth used in coastal cultivation structures. However, positioning the structure even deeper (a third case) should be investigated. Therefore, an optimum depth with less drag force over the droppers and ideal water velocity allowing for high filtration rates, and consequently higher mollusc growth, could be determined.

ACKNOWLEDGEMENTS

The authors would like to express their gratitude to the organizers of XXXVIII Iberian Latin-American Congress on Computational Methods in Engineering to hosting the event. Also, we are grateful of CD-adapco for their license bonus given for current work simulations on STAR-CCM+ commercial software and for the Foundation for Research Support of the State of Rio Grande do Sul to found the current research.

REFERENCES

CD-adapco, 2017. *STAR-CCM+ 12.02 User Guide*.

Donncha, F.O., Hartnett, M. & Nash, S., 2013. Physical and numerical investigation of the hydrodynamic implications of aquaculture farms, *Aquacultural Engineering*, vol. 52, pp. 14-26.

Fenton, J.D., 1985. A Fifth-order stokes theory for steady waves, *J. Waterway, Port, Coastal Ocean Eng.*, vol. 111, n. 2, pp. 216-234.

Ferziger, J.H & Perić, M., 2002. *Computational Methods for Fluid Dynamics*, Springer, third edition, ISBN: 3-540-42074-6.

Food and Agriculture Organization, 2017. *An Overview of Recently Published Global Aquaculture Statistic*.

Lin, J., Li, C. & Zhang, S., 2016. Hydrodynamic effect of a large offshore mussel suspended aquaculture farm, *Aquaculture*, vol. 451, pp. 147-155.

Marenzi, A.W.C. & Branco, J.O., 2006. O cultivo do mexilho Perna perna no municpio de Penha, SC. *Bases ecolgicas para um desenvolvimento sustentvel: estudos de caso em Penha, SC*. Ed. UNIVALI, vol. 291, pp. 227-244.

Newell, C.R., Wildish, D.J. & Macdonald, B.A., 2001. The effects of velocity and seston concentration on the exhalant siphon area, valve gape and filtration rate of the mussel *Mytilus edulis*. *Journal of Experimental Marine Biology and Ecology*, vol. 262, pp. 91?111.

Newman, J.N., 1977. *Marine Hydrodynamics*, The MIT Press, ISBN: 978-0-262-14026-3.

Pilditch, C.A. & Grant, J., 1999. Effect of variations in flow velocity and phytoplankton concentration on sea scallop (*Placopecten magellanicus*) grazing rates. *Journal of Experimental Marine Biology and Ecology*, vol. 240, pp. 111-136.

Plew, D.R., 2005. *The Hydrodynamic Effects of Long-line Mussel Farms*. PhD thesis, University of Canterbury, Christchurch, New Zealand.

Plew, D.R., Enright, R.M.P., Nokes, I. & Dumas, J.K., 2009. Effect of mussel bio-pumping on the drag on and flow around a mussel crop rope. *Aquacultural Engineering*, vol. 40, pp. 55-61.

Strohmeier, T., Aure, J., Duinker, A., Castber, T., A. Svardal & Strand, ., 2005. Flow reduction, seston depletion, meat content and distribution of diarrheic shellfish toxins in a long-line blue mussel (Mytilus edulis) farm. *Journal of Shellfish Research*, vol. 24, n.1, pp. 15-23.

Sobral, P. & Widdows, J., 2000. Effects of increasing current velocity, turbidity and particle-size selection on the feeding activity and scope for growth of *Ruditapes decussatus* from Ria Formosa, southern Portugal. *Journal of Experimental Marine Biology and Ecology*, vol. 245, pp. 111-125.

Wilcox, D.C., 2000. *Turbulence Modelling for CFD*, DCW industries, second edition, ISBN:0-9636051-5-1.

Wildish, D.J. & Saulnier, A. M., 1993. Hydrodynamic control of filtration in *Placopecten magellanicus*, *Journal of Experimental Marine Biology and Ecology*, vol. 174, pp. 65-82.